Table 2 Comparison of Space Shuttle specifications with those of Mini Shuttle and Lockheed Martin X-33/VentureStar vehicles

	STS	Mini STS	VentureStar	X-33
Length, ft	184	149	127	67
Width, ft	78	62	128	68
Gross liftoff weight, lb	4,439.000	4,460,000	2,186,000	273,000
Propellant	LH2/LO2 + solid	RP-1/LO2 + solid	LH2/LO2	LH2/LO2
Propellant weight, lb	3,776,600	3,926,900	1,929,000	211,000
Empty weight, lb	619,000	502,000	197,000	63,000
Main propulsion	Two solids + three SSMEs	Two solids + three MSMEs	Seven RS 2200	Two J-2S
Liftoff thrust	6,400,000	6,400,000	3,010,000	410.000
Maximum speed	Orbital	Orbital	Orbital	Mach 15+
Payload weight, lb	42,900	30,900	59,000	NA
Payload bay size, ft	15 × 60	12 × 48	15 × 45	5 × 10
Sea level specific impulse, s[a]	391	300	347	347
Vacuum specific impulse, s[a]	453	359	455	455

[a]Liquid rocket engine.

and is intended to be a technology demonstrator. Inasmuch as it is designed for suborbital operation, the ratio of structural weight to fully loaded weight is not critical. However, this is just the opposite with the VentureStar vehicle. According to its specifications, this SSTO vehicle will have an empty weight of 197,000 lb and a propellant load at liftoff of 1,929,000 lb. Assuming the same mixture ratio of 6 for oxidizer mass to fuel mass as used for the Shuttle's main engines, the volume of propellant tankage required is 638,220 gal. This is compared to the 518,000-gal capacity of the Shuttle's ET. It presents a very formidable, if not impossible, design problem then to build a practical spacecraft of such voluminous size that weighs only about 30% more than the Shuttle Orbiter. With consideration of these facts and other negative aspects, it is difficult to understand the arguments for feasibility presented by proponents of the SSTO concept.[2,3]

Conclusions

From a preliminary analysis for feasibility of a kerosene-fueled Mini Shuttle, it appears that this type of launch vehicle could be a practical solution to the problem of finding a worthy replacement for the Space Shuttle. Because no new technology is required, there would probably be greater safety and less risk than with other proposed systems such as the SSTO VentureStar. Moreover, the development time would be considerably shorter with greater assurance of meeting performance objectives. Although it is difficult to estimate precisely the reduction in launch costs with the Mini Shuttle, the savings should be substantial. With a $\frac{4}{5}$-size Orbiter, a $\frac{3}{4}$-size ET, and the same SRBs, the Mini Shuttle would have a payload capability about 75% of the Space Shuttle. Thus, there would seem to be sufficient justification for NASA to undertake an in-depth study of the merits of combining the Mini-Shuttle concept with that of the Shuttle II.

References

[1]Bekey, I., Powell, R., and Austen, R., "NASA Studies Access to Space," *Aerospace America*, Vol. 32, No. 5, 1994, pp. 38–43.

[2]Bekey, I., "SSTO Rockets: A Practical Possibility," *Aerospace America*, Vol. 32, No. 7, 1994, pp. 32–37.

[3]Austen, R. E., and Cook, S. A., "SSTO Rockets: Streamlining Access to Space," *Aerospace America*, Vol. 32, No. 11, 1994, pp. 34–38.

[4]Dornheim, M. A., "Follow-on Plan Key to X-33 Win," *Aviation Week and Space Technology*, July 1996, pp. 20–23.

[5]Eldred, C., and Powell, R., "NASA's Baseline Design for New Space Transportation System," AIAA Paper 95-9275, Jan. 1995.

[6]Berry, J., "Design Drivers for Cost-Effective Single-Stage-to-Orbit Vehicles," AIAA Paper 95-0278, Jan. 1995.

[7]Urie, D., "Lockheed's Perspective on Single-Stage-to-Orbit Vehicle Concept," AIAA Paper 95–0279, Jan. 1995.

[8]Pack, C., Menees, G. P., Bowles, J. V., Lawrence, S. L., and Davies, C. B., "Bent Biconic Single-Stage-to-Orbit Conceptual Study," *Journal of Spacecraft and Rockets*, Vol. 33, No. 4, 1996, pp. 470–475.

[9]Nelson, D. A., "The Case for Shuttle II," *Aerospace America*, Vol. 31, No. 11, 1993, pp. 24–27.

[10]Boltz, F. W., "Mini Shuttle: A More-Economical RLV," Author, 1996.

[11]Boltz, F. W., "Analytical Method for Studying the Motion and Mass Loss of Ballistic Rockets Launched Into Orbit," Author, 1996.

[12]Sarner, S. F., *Propellant Chemistry*, 1st ed., Reinhold, New York, 1966, pp. 86, 87.

J. A. Martin
Associate Editor

Aerodynamic Flight Measurements and Rarefied-Flow Simulations of Mars Entry Vehicles

Robert C. Blanchard,* Richard G. Wilmoth,† and James N. Moss‡
NASA Langley Research Center, Hampton, Virginia 23681-0001

Introduction

IN 1976, two Viking spacecraft successfully landed on Mars. The Viking Lander 1 touched down on the Martian surface (22.5°N, 48°W) about 4 p.m. local solar time on July 20, 1976, and later that year on Sept. 3, Viking Lander 2 landed (44°N, 226°W) about 10 a.m. local solar time. During entry, both vehicles traversed all of the speed regimes going from orbital velocities under near vacuum conditions, i.e., the free-molecule flow regime, through the hypersonic noncontinuum and continuum regimes, down to zero velocity on the planet's surface, where the pressure of the CO_2 atmosphere is less than 1% of the Earth's surface pressure. Because of the tenuous Martian atmosphere, a three-tier deceleration system (aerodynamic braking, drag magnification using a parachute, and finally terminal descent landing rockets) was used to place the Viking science payload on the surface of the planet. The Viking aerodynamic braking phase used a spherically blunted, 70-deg half-angle cone entry vehicle. Viking 1 was designated as the pathfinder for the second identical entry vehicle. Data collected from the first entry were quickly processed[1] and analyzed so that full advantage could be taken of the knowledge gained from the first Mars entry experience. This initial analysis was followed by more detailed analysis of the atmosphere[2] as well as vehicle performance.[3]

Received March 18, 1997; revision received June 24, 1997; accepted for publication June 26, 1997.

*Senior Research Engineer, Aerothermodynamics Branch. Associate Fellow AIAA.

†Senior Research Engineer, Aerothermodynamics Branch. Senior Member AIAA.

‡Senior Research Engineer, Aerothermodynamics Branch. Fellow AIAA.

Two spacecraft are scheduled to arrive at Mars on July 4 (Pathfinder mission[4]) and Sept. 12, 1997 (Mars Global Surveyor mission[5]). The Pathfinder mission will place a remotely controlled rover vehicle on Mars' surface. The Pathfinder's multiple deceleration systems are similar to those used by the Viking entry vehicles with the addition of an air bag to cushion the touchdown. Also, like the Viking mission, the first stage of deceleration employs a spherically blunted, 70-deg half-angle cone entry vehicle. However, the entry speed of Pathfinder is nearly twice that of Viking due to the direct entry on the Earth–Mars transfer, as opposed to Viking's deorbit from an existing orbit about Mars. The Mars Global Surveyor Orbiter includes the use of aerobraking to circularize the orbit about Mars prior to conducting various scientific mapping surveys.

In addition, the near future mission to Mars, Mars 2001, includes plans for a direct aerocapture transfer from the Earth–Mars trajectory. The planned vehicle shape is also a spherically blunted, 70-deg half-angle cone. All of these, and future aerobraking missions to Mars, rely on knowledge of the entry vehicle aerodynamic characteristics as it transitions from the free-molecule flow regime into the hypersonic continuum regime, as well as knowledge of the properties of the upper atmosphere. Typically, wind-tunnel data are not available in the rarefied regime so that designers rely heavily on computational results. Confidence can be greatly enhanced by comparing the flight data, in lieu of wind-tunnel data, to computational results. Fortunately, for Mars, the wealth of data collected by the Viking missions provides confidence to the design of future Mars missions. The purpose of this Note is to present a comparison of Viking 1 flight aerodynamic extraction results with recent direct simulation Monte Carlo (DSMC) simulations in the rarefied-flow regime. An application of the DSMC codes to calculate the Pathfinder entry vehicle aerodynamic drag is also shown.

Attitude and Density Results

The Viking entry vehicle was instrumented with three-axis accelerometers and gyros, a mass spectrometer, stagnation pressure sensor, and other scientific instruments. For this brief Note, only those measurements germane to the aerodynamic coefficients will be discussed. Other data and more detailed results exist in the open literature.[1–3]

From the gyro measurements, the attitude of the entry vehicle can be obtained, and it is shown in Fig. 1 as a function of altitude for Viking 1. Positive lift is generated with a negative angle of attack, i.e., vehicle nose down relative to the velocity vector, for a spherically blunted, 70-deg half-angle cone entry vehicle. The Viking mission used lift to prolong the atmospheric transit time during the aerobraking phase to maximize the dissipation of the vehicle's kinetic energy. Above about 75 km, the onboard control system was programmed to hold a constant attitude of approximately 11 deg. At 0.05 g, which was sensed by the accelerometers, the attitude control system was programmed to switch to an attitude rate damping mode for the remainder of the aerobraking phase. This event occurred at about 75 km (Fig. 1). Viking 1 trimmed at about 10.7 deg, an angle just slightly less than the design value of 11 deg (Fig. 1) at altitudes from about 40–50 km. The attitude information shown in Fig. 1 will be an important reference when interpreting the aerodynamic coefficients shown later.

The Viking measurements are used to generate the density encountered by the vehicle. The sources for density from flight are the mass spectrometer, the stagnation pressure sensor, and the accelerometers. The Viking mission had an open-source magnetic-sector mass spectrometer as part of its scientific complement.[6] The pressure device senses pressure by deflection of a thinly stretched diaphragm referenced to a vacuum chamber and is also part of the complement of scientific instruments. The accelerometers were used for both engineering purposes, e.g., guidance and control, as well as part of the scientific complement in generating the atmospheric state properties. Figure 2 shows the density–altitude profile derived from the measurements of the mass spectrometer at higher altitudes and the stagnation pressure sensor and accelerometers at lower altitudes. Between about 110 and 130 km, the noise on the accelerometers and

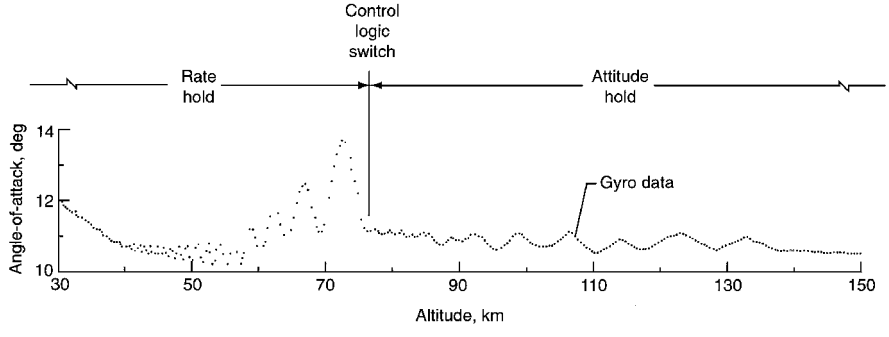

Fig. 1 Viking 1 vehicle angle of attack vs altitude during transition into hypersonic continuum from free-molecule flow.

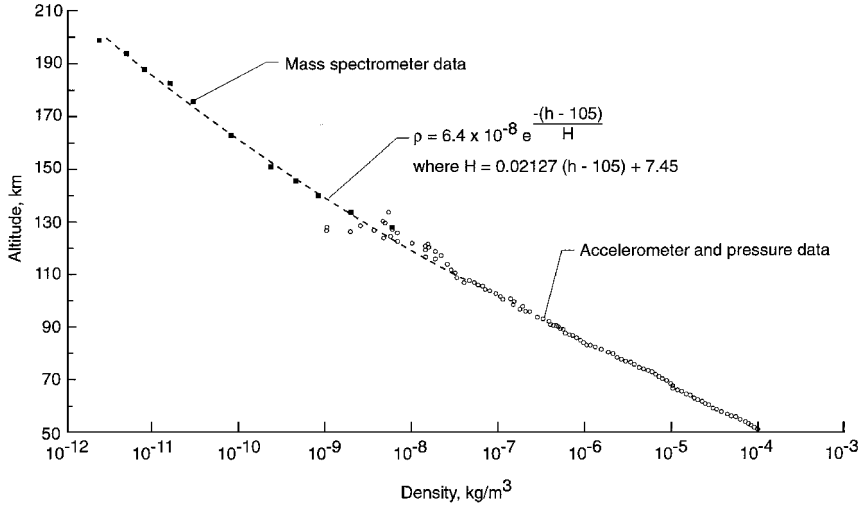

Fig. 2 Atmospheric density vs altitude from Viking 1 measurements.

the reliability of the corrections to the mass spectrometer data leave a gap between the data sets. A fit to both sets of data is used to bridge this data gap. The function used for the fit, the values obtained for the function constants, and the resulting comparison with the data (the dashed line) are shown in Fig. 2.

Aerodynamic Results

Extracting individual coefficients from acceleration requires a knowledge of atmospheric density. When this is not available, the most reliable aerodynamic measurements are obtained by establishing acceleration ratios inasmuch as dynamic pressure cancels and the acceleration ratio is identical with the force coefficient ratio. The ratio of acceleration measurements (normal to axial direction) for Viking 1 as a function of altitude is presented in Fig. 3. This measurement corresponds to the hypersonic continuum regime at about 11-deg angle of attack for altitudes less than about 70 km and the transition into the rarefied-flow regime at altitudes larger than 70 km. Above about 110 km, the accelerometer noise begins to dominate prior to achieving the free-molecule flow regime.

Using the already discussed information on the vehicle attitude, i.e., the density derived from mass spectrometer, pressure sensor, and acceleration measurements along with other information, e.g., velocity, given in Ref. 3, three-dimensional DSMC simulations[7] were performed for selected trajectory points. The results of these calculations are shown in Fig. 3. The DMSC predictions for the rarefied-flow transition region show excellent agreement with the flight measurements. Free-molecule flow results assuming complete diffuse reflection (applicable to near orbital conditions) and modified Newtonian results for the hypersonic continuum conditions are included in Fig. 3.

Previous work with the Viking 1 data, reported in Ref. 3, allowed for a separation of the drag coefficient C_D from density using the stagnation pressure sensor measurements. However, this analysis was limited to the hypersonic continuum regime (altitudes less than about 70 km) due to the capability of the pressure sensor. Figure 4 shows these flight results, together with the corresponding six points from the DSMC simulations for Viking 1. In addition, the corresponding free-molecule flow and modified Newtonian values are included. In essence, Fig. 4 shows the complete aerodynamic drag of the spherically blunted, 70-deg half-angle cone entry vehicle from free-molecule flow down into the hypersonic continuum at an angle of attack of about 11 deg.

The Pathfinder entry vehicle, also a spherically blunted, 70-deg half-angle cone shape but with a slightly different afterbody, has been simulated at 0-deg angle of attack with a two-dimensional DSMC code.[8] Both vehicles have the same bluntness ratio (nose to aft radius) of 0.5. The results of the simulation are also included for comparison in Fig. 4. To make the appropriate comparison of the Pathfinder calculations on an altitude basis, the density profile measured by Viking 1 was used. For a given altitude, both the Viking and Pathfinder simulations used the same density and also the same composition (95.37% CO_2 and 4.63% N_2 mole fractions). The Pathfinder vehicle angle of attack is nominally 0 deg, and thus it is expected that the hypersonic continuum values should be larger than the Viking results for 11 deg. Notice, at about 70 km, that the Pathfinder DSMC results tend to level out at a drag coefficient that is larger than the Viking flight measured values, as expected. At the other extreme, for altitudes above 120 km, the Pathfinder free-molecule flow values differ only slightly from the Viking 1 results. It is difficult to make a direct comparison between the two entry missions near the free-molecule flow regime for several reasons. The rarefaction effect on Pathfinder is slightly larger than Viking because the Viking vehicle diameter is larger (3.50 vs 2.65 m). Also, the Pathfinder vehicle entry speed is larger than Viking entry speeds. Further, the variation in C_D with angle of attack in the continuum is different from the variation in the free-molecule flow regime. The

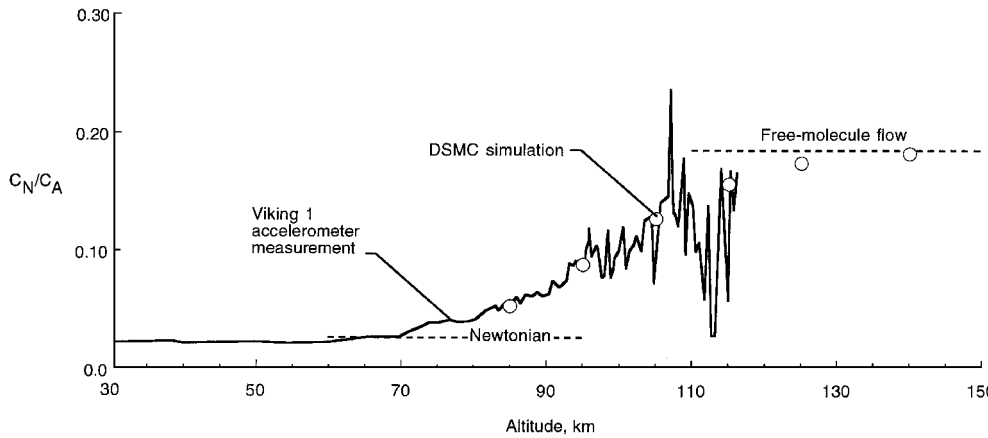

Fig. 3 Normal-to-axial coefficient derived from Viking 1 acceleration measurements compared with DSMC simulations.

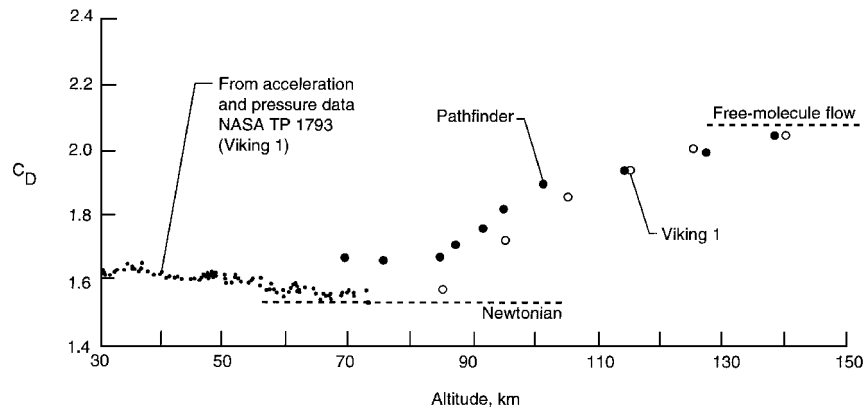

Fig. 4 Viking 1 drag coefficient vs altitude from flight measurements and DSMC simulation, along with Pathfinder drag coefficient predictions from DSMC simulations.

main point is that, with the success in matching the DSMC simulations with the Viking flight data, there is renewed confidence that the simulations for the Pathfinder vehicle are correct.

Summary

The normal-to-axial force coefficient ratio of the Viking spherically blunted, 70-deg half-angle cone entry vehicle has been extracted from flight data in the transition from the hypersonic continuum into the free-molecule flow transition regime. Results from simulations of the Viking vehicle with a three-dimensional DSMC code show an excellent match with the flight data. DSMC simulations of the Pathfinder entry into Mars have been computed to the fringes of the hypersonic continuum flight regime. The drag coefficients for this mission are compared to the Viking simulation with good qualitative agreement, thereby providing reinforcement that the DSMC codes are reliably providing appropriate aerodynamic characteristics in the rarefied-transitional flow flight regimes.

References

[1]Euler, E. A., Adams, G. L., and Hopper, F. W., "Design and Reconstruction of the Viking Lander Descent Trajectories," *Journal of Guidance and Control*, Vol. 1, No. 5, 1978, pp. 372–378.

[2]Seiff, A., and Kirk, D. B., "Structure of the Atmosphere of Mars in Summer at Mid-Latitudes," *Journal of Geophysical Research*, Vol. 82, No. 28, 1977, pp. 4364–4378.

[3]Blanchard, R. C., and Walberg, G. D., "Determination of the Hypersonic-Continuum/Rarefied-Flow Drag Coefficient of the Viking Lander Capsule I Aeroshell from Flight Data," NASA TP 1793, Dec. 1980.

[4]Spears, A. J., Freeman, D. C., Jr., and Braun, R. D., "Mars Pathfinder Status at Launch," 47th International Astronautical Congress, International Astronautical Federation, Paper No. IAF-96-Q.3.02, Oct. 1996.

[5]Dallas, S. S., "Mars Global Surveyor Mission," *Proceedings of 1997 IEEE Aerospace Conference*, Vol. 4, Inst. of Electrical and Electronics Engineers, New York, 1997, pp. 173–189.

[6]Nier, A. O., and McElroy, M. B., "Composition and Structure of Mars' Upper Atmosphere: Results from the Neutral Mass Spectrometer on Viking 1 and 2," *Journal of Geophysical Research*, Vol. 82, No. 28, 1977, pp. 4341–4349.

[7]Wilmoth, R. G., LeBeau, G. J., and Carlson, A. B., "DSMC Grid Methodologies for Computing Low-Density Hypersonic Flows About Reusable Launch Vehicles," AIAA Paper 96-1812, June 1996.

[8]Bird, G. A., "The G2/A3 Program System Users Manual," G. A. B. Consulting Pty Ltd., Killara, New South Wales, Australia, March 1992.

I. D. Boyd
Associate Editor